Biophysical Chemistry 5 (1976) 185–196


# SEDIMENTATION EQUILIBRIUM TECHNIQUES: MULTIPLE SPEED ANALYSES AND AN OVERSPEED PROCEDURE

Dennis E. ROARK

*Department of Biological Chemistry, The Milton S. Hershey Medical Center, The Pennsylvania State University, Hershey, PA 17033, USA*

The use of a single high-speed sedimentation equilibrium experiment to analyze mixed associating systems is inadequate to determine the association mode even if the molecular weight of one species is known. Simultaneous analysis of the concentration distributions at three equilibrium speeds greatly reduces the lack of uniqueness. Linear least-squares multi-speed fits discriminate between association models in which the molecular weights are assumed. Experiments at a series of initial concentrations as well as rotor speeds further increases the discrimination.

An overspeed procedure is proposed. The overspeed time depends only slightly on the sedimenting species molecular weight, but significantly on the frictional ratio. A minimal overspeed time may be estimated.

## 1. Introduction

Perhaps the most powerful future application of sedimentation equilibrium experiments is the study of associating systems. The ultracentrifuge is capable not only of determining the existence of oligomeric species but of studying the equilibrium thermodynamics of reversible, rapidly equilibrating associations. In contrast, the use of cross-linking agents followed by analytical gel electrophoresis can give only qualitative information in the proximity of polypeptide chains and not on the nature of the interactions. Analyses of moving boundaries in sedimentation velocity or in gel permeation chromatography are often powerful techniques for the study of interactions. But these methods are seriously complicated by their non-equilibrium nature: particle shape and various hydrodynamic nonidealities are reflected in the data. Thus, sedimentation equilibrium remains of great promise in the exploration of associating systems.

A collection of ideally behaving species at sedimentation equilibrium produces a concentration distribution that is a sum of exponentials:

$$c(r) = \sum_i A_i \exp(\sigma_i r^2/2), \tag{1}$$

where $r$ is the radius, $\sigma_i$ is the reduced molecular weight [1]

$$\sigma_i = M_i(1-\bar{v}_i\rho)\omega^2/RT, \tag{2}$$

for a species of molecular weight $M_i$ and partial specific volume $\bar{v}_i$ sedimenting in a solution of density $\rho$ and temperature $T$ at an angular velocity $\omega$. The problem posed by sedimentation equilibrium analyses is the estimation of the amplitude $A_i$ and reduced molecular weight $\sigma_i$ from the concentration distribution $c(r)$. The unique solution of this problem for a sum of exponentials is notoriously difficult in all but the simplest cases. For each species assumed present, two degrees of freedom are contributed to the analysis. In a careful consideration of increasing degrees of complexity, Haschemeyer and Bowers [2] concluded that not more than 5 degrees of freedom can be uniquely analyzed under favorable experimental situations. Thus, in the study of mixed-associations, which necessarily involve three or more species, a single sedimentation equilibrium experiment provides inadequate information for a unique analysis. Additional information is often available from other experiments; and, for instance, the molecular weights of one or more species may be known, thereby reducing the degrees of freedom of the problem at hand.

In this paper we examine the use of combining sedimentation equilibrium experiments at different speeds in a single analysis to reduce the ambiguity of the analysis. Multiple-speed analysis was used by Scholte [3] in his noteworthy technique for determin-

ing a molecular-weight-distribution function for a collection of non-interacting species. We find here, as well, that simultaneous multi-speed analysis permits resolution of problems that have non-unique solutions at any one speed. We also offer a tentative re-evaluation of the possibilities of overspeeding a high-speed equilibrium experiment to reduce the total time required to essentially achieve equilibrium.

## 2. Distinguishing association modes

Experimental necessity dictated the development of the technique described in the next section. We have been concerned with associative interactions among the arginine-rich histones f2a1 and f3 from calf thymus [4]. Our studies and those of Kornberg [5] suggest that these histones are the subunits of the mixed tetramer $(f2a1)_2(f3)_2$. Furthermore, sedimentation equilibrium studies indicate that this tetramer dissociates to a "dimer", as shown by the "two-species plot" [6] of fig. 1. Histones f2a1 and f3 have sequence determined molecular weights of 11 240 and 15 320, respectively [7,8]. Two dissociation modes of the 53 120 m.w. tetramer are possible:

$$(f2a1)_2 + (f3)_2 \rightleftharpoons (f2a1)_2(f3)_2, \quad (3)$$

$$2(f2a1)(f3) \rightleftharpoons (f2a1)_2(f3)_2. \quad (4)$$

The dimer of eq. (4) has a m.w. of 26 560; while the $(f2a1)_2$ and $(f3)_2$ dimers of eq. (3) have m.w.'s of 22 480 and 30 640, respectively. Eq. (4) involving the dimerization of the mixed dimer is a homogeneous self-associating system; while eq. (3) describes a heterogeneous or mixed association. In principle, the homogeneous and heterogeneous associations can be distinguished by comparison of equilibrium experiments at different initial loading concentrations or rotor speeds [1,6]. For a series of initial loading concentrations, heterogeneous association results in non-overlap of presentations of any molecular weight moment such as $\sigma_w$ (reduced weight-average molecular weight) as a function of local equilibrium concentration. For a series of rotor speeds, an analogous presentation of $\sigma_w/\omega^2$ versus local equilibrium concentration yields non-overlapping curves for a heterogeneous

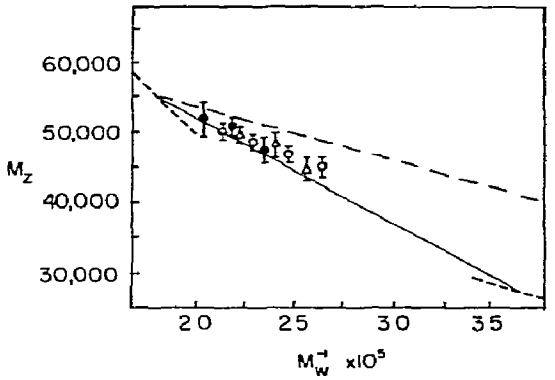


Fig. 1. "Two-species" plot for f2a1–f3. Association behavior presented as $M_z(r)$ a function of $M_w^{-1}(r)$ for three loading concentrations: (•) 0.2 mg/ml; (○) 0.6 mg/ml; and (△) 1.8 mg/ml. Sedimentation equilibrium conditions are 0.05 M NaOAc, 0.05 M $NaHSO_3$, 0.005 M EDTA, pH 5; 20°C; and 34 000 rpm. Solid line represents a monomer-dimer equilibrium, while dashed line represents a monomer-tetramer equilibrium. Portions of the hyperbola, $M_z(1/M_w) = 1$, are shown as the heavy deshed line.

system. However, the ability to detect significant non-overlap depends upon the estimated error of the values of $\sigma_w$.

To determine if apparent overlap of $\sigma_w$ versus concentration curves for the histone association experiments demonstrated the self-association mode of eq. (4), computer simulations were performed. The problem involves distinguishing the association modes of eqs. (5) and (6)

$$A + B \rightleftharpoons C, \quad (5)$$

$$2A' \rightleftharpoons C, \quad (6)$$

in which the molecular weight of species A′ is the mean of species A and B. Figs. 2 and 3 present $\sigma_w$ as a function of local equilibrium concentration for the mixed association of eq. (5). Simulated conditions were those typically employed in high-speed sedimentation equilibrium experiments. Fig. 2 presents a simulation in which the sigma's of species A, B and C are 4, 6 and 10 $cm^{-2}$, respectively. These ratios of molecular weights correspond approximately to the mixed histone association of eq. (3). As can be seen, the non-overlap is slight and would not be detected in an actual

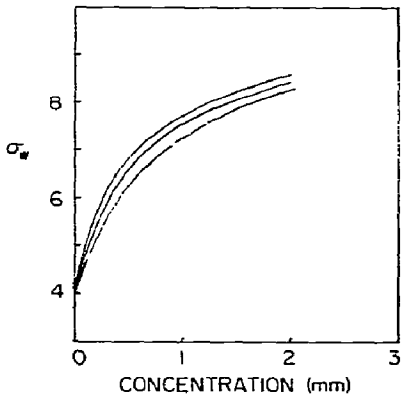


Fig. 2. Association behavior with a series of loading concentrations for a mixed-associating system with $\sigma$'s 4, 6 and 10 $cm^{-2}$. Simulated loading concentrations are 0.75, 1.5 and 3 mm fringe displacement. Association constant is 5 $mm^{-1}$. Column length is 0.36 cm.

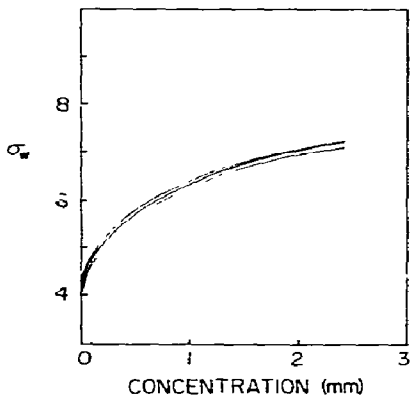


Fig. 3. Association behavior with a series of loading concentrations for a mixed-associating system with $\sigma$'s 4, 8 and 12 $cm^{-2}$. Other conditions are those of fig. 2.

experiment. Greater non-overlap is apparent in fig. 3, where species A, B and C have sigmas of 4, 8 and 12 $cm^{-2}$, respectively. This non-overlap is probably just adequate for detection in experimental data. Thus, the self and mixed-association modes of eqs. (5) and (6) cannot be distinguished on the basis of apparent heterogeneity unless species B is at least twice as large as species A. The use of a series of rotor speeds rather than a series of loading concentrations is even less sensitive to heterogeneity. Fig. 4 presents a rotor speed series for the system of fig. 3. The speed ratios are 1:1.189:1.414, spanning a twofold range of sigma.

An alternative to the local molecular weight average analyses described above is the direct fit of the concentration distribution by a sum of exponentials. Such fits can be of two classes: with and without chosen models. Linear least-squares analyses may be performed to determine the amplitudes $A_i$ if the $\sigma_i$ have been previously chosen to correspond to some model. Examination of the residuals or standard deviation of the fit is then useful to determine the correctness of the model. If two models cannot be distinguished on the basis of their residuals, non-linear least-squares fits of the same data will necessarily be ambiguous and unstable to small perturbations of random errors.

Simulated concentration distributions were generated for the mixed-association mode of eq. (5). Concentrations, measured in mm of fringe displacement, were perturbed by 0.003 mm ($3\mu$) normally-distributed random noise. Local concentrations having gradients greater than those normally observed in an experiment were deleted. The gradient limit corresponds to $c\sigma_w = 18$. These simulated concentration distributions were then analyzed by least-squares analysis assuming the monomer–dimer self-association mode of eq. (6). Table 1 presents the standard deviations of these fits for several simulated conditions. All standard deviations have been normalized by dividing by the $3\mu$ standard deviation of the contributed ran-

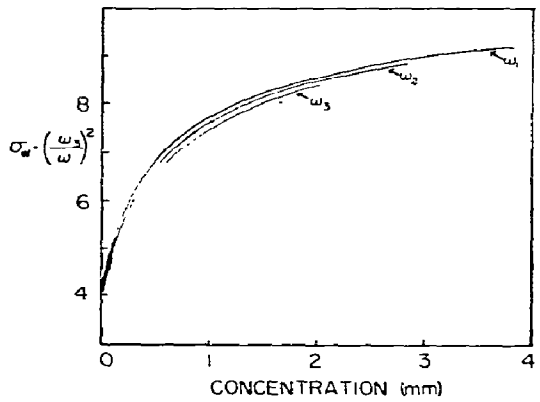


Fig. 4. Association behavior with a series of rotor speeds for a mixed-associating system. At the highest speed, $\omega_3$, $\sigma$'s are 4, 8 and 12 $cm^{-2}$. Speed ratios are 1:1.189:1.414. Initial loading concentration is 1.5 mm; association constant is 5 $mm^{-1}$; and column length is 0.36 cm.

Table 1
Least-squares fits of mixed-associations by a self-association model

| $A + B \rightleftharpoons C$ [a] σ's | $\Delta r$ [b] | $2A' \rightleftharpoons C$ [c] n.S.D. |
|---|---|---|
| 2, 3, 5 $cm^{-2}$ | 0.36 cm | 1.3 |
| 4, 6, 10 | 0.36 | 1.3 |
| 2, 3, 5 | 0.72 | 2.0 |
| 4, 6, 10 | 0.72 | 1.7 |
| 4, 8, 12 | 0.36 | 3.0 |

a) Simulated, noise perturbed model with $K = 5$ $mm^{-1}$ and $c_{total} = 1.5$ mm fringe displacement.
b) Meniscus to base distance.
c) Normalized standard deviations (S.D./3$\mu$) for least-squares fits assuming monomer–dimer model with $A' = (A+B)/2$.

dom noise. The incorrect model of eq. (6) cannot be excluded by the least-squares analysis unless the normalized standard deviation (n.S.D.) is sufficient. A reasonable criterion is that the n.S.D. be 3 or greater. The present quality of "blank pattern correction" reproducibility contributes small systematic errors to the fringe patterns. This, plus the small errors obtained even with automated plate readers [9], suggests the appropriateness of requiring standard deviations of at least 9$\mu$ if a fit is to demonstrate the inadequacy of an assumed model. The data of table 1 demonstrate that the mixed-association and self-association cannot be distinguished if the sigmas of species A, B and C are 4, 6 and 10 $cm^{-2}$, respectively. The inadequacy of the least-squares analysis of this system is independent of rotor speed or column length: the normalized standard deviation increases only slightly for 0.72 cm meniscus-to-base distance. In agreement with the ability to detect heterogeneity by presentations of $\sigma_w$ as a function of concentration, only if species B is twice the molecular weight of species A can the standard deviation of the fit detect the inconsistency of the assumed self-association model.

## 3. Simultaneous multiple speed analyses of sedimentation equilibrium experiments

To resolve the ambiguities often inherent in the least-squares fit of a single concentration distribution, simultaneous fits of several concentration distributions of the same system but at differing rotor speeds or initial loading concentrations may be made. Simplicity is possible if the least-squares procedure remains linear. The method described here simultaneously fits distributions for a series of speeds by a linear procedure.

For convenience, we describe the concentration distribution by

$$c(\xi) = \sum_i c_{0_i} \Gamma_i(\xi, \sigma_i), \tag{7}$$

where $\xi$ is $r^2/2$; $c_{0_i}$ is the (hypothetical, for an interacting system) initial loading concentration of species $i$, or alternatively, the mean concentration of species $i$; and the position parameters $\Gamma$ are

$$\Gamma_i(\xi, \sigma_i) = \frac{\sigma_i(\xi_b - \xi_m)\exp[\sigma_i(\xi - \xi_b)]}{1 - \exp[-\sigma_i(\xi_b - \xi_m)]}, \tag{8}$$

where $\xi_m$ and $\xi_b$ correspond to the meniscus and base of the cell.

The mixed-association mode, eq. (5), has a concentration distribution at sedimentation equilibrium:

$$c(\xi) = c_{0a}\Gamma_a(\xi) + c_{0b}\Gamma_b(\xi) + c_{0c}\Gamma_c(\xi). \tag{9}$$

The mean species concentrations, $c_{0a}$, $c_{0b}$ and $c_{0c}$, of this associating system depend on initial loading concentrations of the three species and on the angular velocity $\omega$, such that mass action is obeyed at all points in the cell. (We assume mass action to be obeyed on a concentration basis and neglect variations in the solute activity coefficients. In addition, the equilibrium constant is assumed independent of pressure.) Thus, for this association, the equilibrium constant $K$ on a weight concentration basis is

$$K = \frac{c_{0c}\Gamma_c(\xi)}{c_{0a}c_{0b}\Gamma_a(\xi)\Gamma_b(\xi)}. \tag{10}$$

Although the mean species concentrations are functions of rotor speed (since the $\Gamma$ are functions of speed) the total amounts of components A and B are speed invariant. Component A is partially present as species A and the remainder as a weight fraction of species C. Thus, we may define the "total mean component concentrations" of A and B, $c_{aT}$ and $c_{bT}$:

$$c_{aT} \equiv c_{0a} + (\sigma_a/\sigma_c)c_{0c_i}, \tag{11}$$

$$c_{bT} \equiv c_{0b} + (\sigma_b/\sigma_c)c_{0c_i} \tag{12}$$

The total mean concentrations $c_{aT}$ and $c_{bT}$ are speed invariant and are therefore useful fitting parameters

for simultaneous multi-speed fits. Eqs. (9), (11) and (12) may be combined to replace $c_{0a}$ and $c_{0b}$ by $c_{aT}$ and $c_{bT}$:

$$c(\xi) = c_{aT}\Gamma_a + c_{bT}\Gamma_b + c_{0c_i}[\Gamma_{c_i} - (\sigma_a/\sigma_c)\Gamma_a - (\sigma_b/\sigma_c)\Gamma_b]. \quad (13)$$

Eq. (13), rather than eq. (9), is used to perform simultaneous multi-speed fits. If values of $\sigma_a$, $\sigma_b$ and $\sigma_c$ are previously chosen, then the fitting parameters are $c_{aT}$, $c_{bT}$ and the $c_{0c_k}$ for speeds $k$. Thus, a fit of a single speed has three degrees of freedom; while a simultaneous fit of three speeds would have five degrees of freedom. These five degrees constitute a significant restriction compared to the nine degrees of freedom if each speed were separately analyzed. The reduction of degrees of freedom (per channel) makes possible a more unique analysis. By constraining $c_{aT}$ and $c_{bT}$ to be the same at all three speeds, the separate concentration distributions serve as mutual constraints in the fit.

The three speeds (or any number of speeds) can be easily combined into a single least-squares analysis by renumbering the concentration and position coordinates. Thus, if the three channels of data representing the same system at three speeds, have $N$, $M$ and $L$ data points, respectively, we combine the data in the following manner:

$$c(\xi_i) = c_{aT}\Gamma_1 + c_{bT}\Gamma_2 + \sum_{k=1}^{3} c_{0c_k}\Gamma_{3k}, \quad (14)$$

for $i = 1, \ldots, N, N+1, \ldots, N+M, N+M+1, \ldots, N+M+L$,

where

$$\Gamma_1 = \Gamma_a, \quad (15a)$$

$$\Gamma_2 = \Gamma_b, \quad (15b)$$

$$\Gamma_{3k} = \Gamma_{c_i} - (\sigma_a/\sigma_{c_i})\Gamma_a - (\sigma_b/\sigma_{c_i})\Gamma_b, \quad (15c)$$

for $i = 1, \ldots, N$ if $k=1$,
$i = N+1, \ldots, N+M$ if $k=2$,
$i = N+M+1, \ldots, N+M+L$ if $k=3$,

$$\Gamma_{3k} = 0, \quad \text{otherwise.} \quad (15d)$$

The $\Gamma$ are functions of $\xi_i$ and rotor speed. A single over-determined least-squares analysis is then performed for the five fitting parameters over the entire combined data set.

The above procedure has been described for the mixed-association of eq. (5). However, it is easily applicable to any association mode. One need only write the corresponding conservation of mass equation(s) for each interacting component present; and combine these with the concentration distribution relation corresponding to eq. (9). This immediately indicates the appropriate choice of the transformed $\Gamma$, as in eq. (15). A particulary simple case is the self-association mode where $n$ monomers form an oligomer:

$$nA \rightleftharpoons B. \quad (16)$$

Here,

$$c(\xi) = c_{0a}\Gamma_a + c_{0b}\Gamma_b. \quad (17)$$

The total mean component concentration is

$$c_{aT} = c_{0a} + c_{0b}. \quad (18)$$

Thus, the equation to fit is

$$c(\xi) = c_{aT}\Gamma_a + c_{0b}(\Gamma_b - \Gamma_a). \quad (19)$$

Eqs. (19), for each speed $k$, are combined as in eqs. (14) and (15), and a fit performed to determine $c_{aT}$ and the three $c_{0b_k}$. The quality of this fit is evaluated by examination of the overall standard deviation:

$$\text{S.D.}^2 = \frac{\sum_{i=1}^{N+M+L}\left(c(\xi_i) - c_{aT}\Gamma_1 - \sum_{k=1}^{3} c_{0b_k}\Gamma_{2k}\right)^2}{N+M+L-4} \quad (20)$$

or of the standard deviations of the three individual channels.

The multi-speed fit described above constrains the total mean component concentrations to be the same for all speeds. This multi-speed fit is termed a "component-constrained" fit. Additional constraints are possible to further reduce the ambiguity of the fits and allow better discrimination between possible association modes. These increased constraints use information generated by the "component-constrained" fit. Estimation of association constants are made and averaged over the several concentration distributions to provide additional constraint. From the "component-constrained" multi-speed fit described above, values of the $c_{0_i}$ are determined for each speed from the conservation of mass equations, such as eqs. (11), (12) or (18).

For example, a multi-speed fit has assumed a monomer–dimer model [eqs. (16)–(20)]. The fit for

three speeds $k$ determines $c_{aT}$ and the three $c_{0b_k}$. Values of $c_{0a_k}$ and equilibrium constants for each speed $k$ are generated from eqs. (10) and (18):

$$c_{0a_k} = c_{aT} - c_{0b_k}, \tag{21}$$

$$K_k = c_{0b_k}\Gamma_b / c_{0a_k}^2 \Gamma_a^2. \tag{22}$$

The position parameters $\Gamma_a$ and $\Gamma_b$ for speed $k$ may be evaluated at any position $\xi$, but most conveniently at the cell base $\xi_b$. The equilibrium constants are then averaged over the three speeds $k$:

$$\bar{K} = \langle K_k \rangle. \tag{23}$$

This average equilibrium constant is then used to generate the $c_{0_i}$ for each speed. To accomplish this, we define the "transformed" equilibrium constant $K_k'$:

$$K_k' = c_{0b_k}/c_{0a_k}^2 = \bar{K}\,\Gamma_a^2/\Gamma_b. \tag{24}$$

With a value of $K_k'$ and $c_{aT}$, eqs. (18) and (24) are solved simultaneously to determine the unknowns $c_{0a_k}$ and $c_{0b_k}$. The values of the $c_{0a_k}$ and $c_{0b_k}$ determined for the speed $k$ are then used to compute a standard deviation for the concentration distribution fit:

$$\text{S.D.}^2 = \frac{\sum_k \sum_i [c_k(\xi_i) - c_{0a_k}\Gamma_a - c_{0b_k}\Gamma_b]^2}{N+M+L-4}. \tag{25}$$

The sum may be over the data for all three speeds $k$, as in eq. (25), or over a single speed. This technique employs the maximum possible constraint for the several speeds by using only two parameters: $\bar{K}$ and $c_{aT}$. The fit is termed "$\omega$-constrained".

In addition to performing experiments at a series of rotor speeds, a multichannel cell [10] permits experiments at three initial loading concentrations. With these three concentrations, sedimentation equilibrium is attained at three rotor speeds. For each concentration channel $j$, the multi-speed analysis is separately performed to determine the mean total component concentrations. For example, the assumed monomer–dimer mode would generate values of $c_{aT_j}$ and $K_{k_j}$ for each concentration $j$. The equilibrium constants are now averaged over speed and loading concentration:

$$\bar{K} = \langle K_{k_j} \rangle. \tag{26}$$

Using this average equilibrium constant and values of $c_{aT_j}$, values of the $c_{0_i}$ are determined, along with the resulting standard deviation of eq. (25). The sum of eq. (25) may be over both speed and loading concentration. This technique is called "$\omega,c$-constrained" and, in terms of model discrimination, is the most powerful considered.

A computer program is available from the author to perform the multi-speed analyses. The program functions either with three sets of experimental data for the three rotor speeds, or by simulating data for a model system. In the simulation mode, one chooses the model, meniscus-to-base distance, initial loading concentrations, equilibrium constants and rotor speeds. The program then simulates the concentration distributions attained at sedimentation equilibrium for the three speeds, terminates simulated data at the gradient limit $c\sigma_w = 18$, and perturbs all data with $3\mu$ normally-distributed random noise. Experimental or simulated data is then analyzed according to a chosen model. Some program changes are required by change of model. Such changes are minimal and are grouped for convenience. All least-squares analyses are accomplished by generating an augmented coefficient matrix which is solved by Crout reduction [11]. This procedure is efficient and permits analysis with any degree of freedom. An additional degree of freedom in all fits is an additive constant corresponding to the choice of concentration zero level in each concentration distribution. The lowest rotor speed generally does not lead to meniscus depletion and therefore requires determination of the zero level by the fit. The extensive depleted regions at the higher speeds provide greatly overdetermined information for the additive fitting constants. The program first fits each speed separately and presents the three standard deviations of these fits. The multi-speed fit is performed and its S.D. determined. Next, the program calculates equilibrium constants for each speed from the multi-speed fit. The average equilibrium constant then is used to calculate an overall S.D. for the $\omega$-constrained fit, as well as individual S.D.'s for each speed. If the $\omega,c$-constrained analysis is desired, the program described is run separately on multi-speed data of three loading concentrations. One then averages the three resultant $\bar{K}$ and enters this overall $\bar{K}$ into the program to generate the standard deviations.

## 4. Multi-speed analyses results

The advantages gained by the multi-speed analysis depend on adequate choice of the three equilibrium speeds and other experimental conditions. In general, the optimal speeds, loading concentrations, and column length are inter-related. Higher speeds require reduced loading concentrations and permit reduced column length. Longer columns generally yield greater resolution of the analysis, in terms of a larger S.D. for an inconsistent model. The column lengths employed in the external loading multi-channel cell are usually from 0.3 to 0.36 cm. The optimal column length is probably about 0.6 cm. (Lengths greater than this merely offer greater meniscus depletion regions for the speeds required here and are of little advantage,) The advantages of using three loading concentrations to perform a $\omega$,$c$-constrained multi-speed fit, outweigh the less than optimal column lengths; and these fits show greater discrimination than do the $\omega$-constrained fits with longer column lengths. An additional advantage in the shorter column lengths accrues in the reduced time required to attain equilibrium. For column lengths near 0.36 cm, the best choice of speeds appears to follow the rationale: choose the lowest speed so that the highest molecular weight species of the assumed model corresponds to $\sigma = 4$ to 6 $cm^{-2}$, and the highest speed so that the lowest molecular weight species has its $\sigma$ in the same range. The intermediate speed is then the geometric mean of the other two speeds. For simulations or experiments at a series of lodaing concentrations, the concentration ratios are chosen to be 1:2:4. The highest initial loading concentration of protein should generally be from 1 to 3 mg/ml.

Gel formation may occur at the cell base in experiments at high sigmas and high concentration. The gel interferes with the multi-speed analysis only if it significantly affects the concentration distribution throughout the cell. Inability to determine the concentration distribution near the cell base where the gel is present does not matter. Thus, to the extent that gel formation is a phase transition above a centain radius and concentration which does not alter the concentration distribution at lesser radii, gel formation represents no problem to the analysis. It is necessary, however, to first approach equilibrium at the lower speeds. To the extent that gel formation represents a disappearance of material from the cell without altering the effective cell base position, only a 2% loss of total cell contents at the highest speed compared to the lowest speed can be tolerated. Gel formation can be reduced by performing experiments at lower speeds and loading concentrations.

Table 2
Multi-speed fits of mixed associations by a self-association model

| $A + B \rightleftharpoons C$ [a] $\sigma$'s | $\Delta r$ | $2A' \rightleftharpoons C$ unconst. | n.S.D. [b] $\omega$,$c$-cont. |
|---|---|---|---|
| 2, 3, 5 $cm^{-2}$ | 0.36 cm | 1.7 | 3.7 |
| 2, 3, 5 | 0.72 | 2.3 | 5.3 |
| 2, 4, 6 | 0.36 | 3.7 | 10.0 |
| 2, 4, 6 | 0.72 | 6.0 | 15.0 |
| 1, 2, 3 | 0.72 | 5.7 | 12.6 |

[a] Simulated mixed-association model is that of table 1.
[b] Normalized standard deviations of single speed (unconstrained) and $\omega$,$c$-constrained multi-speed fits assuming a monomer–dimer model with $A' = (A + B)/2$.

Multi-speed analyses were performed on simulated data corresponding to the mixed association mode of eq. (5). Simulated rotor speeds were in the ratio $1:2^{1/4}:2^{1/2}$, corresponding to a twofold variation of the sigmas. Generally, the smallest species present had a $\sigma$ of 2 $cm^{-2}$ at the lowest rotor speed. Simulated total loading concentrations were 0.75, 1.5, and 3 mm fringe displacement. The simulated data was analyzed assuming the (inconsistent) self-association mode of eq. (6). Normalized standard deviations of 3 were required to detect inconsistency. Table 2 presents the partial results for a set of such analyses. The n.S.D. has been calculated for the nine single speed fits ("unconstrained") and for the none individual concentration distributions using the $\omega$,$c$-constrained fits. The maximum n.S.D. of the nine is presented in each case. If species A and B have sigmas of 2 and 3 $cm^{-2}$, respectively, the unconstrained fit cannot resolve the association mode, as in table 1. The $\omega$,$c$-constrained fit, however, successfully detects the inconsistency in the assumed model. If species B has a molecular weight twice that of species A, both the unconstrained and constrained fits suffice. The n.S.D.'s for the constrained fits are considerably greater. The multi-speed analysis, assuming the monomer–dimer mode, was repeated using simulated monomer–dimer data. In this "control", all constrained and unconstrained

Table 3
Multi-speed fit of $A + B \rightleftharpoons C$ [a] assuming $2A' \rightleftharpoons C$ [b]

| Initial conc. [c] | Speed | n.S.D. [d] | | | |
|---|---|---|---|---|---|
| | | 1 | 2 | 3 | 4 |
| $c_1$ | $\omega_1$ | 1.7 | | 1.7 | 1.7 |
| $c_1$ | $2^{1/4}\omega_1$ | 1.3 | | 1.7 | 1.7 |
| $c_1$ | $2^{1/2}\omega_1$ | 1.7 | | 2.0 | 3.7 |
| $c_1$ | $\{\omega\}$ [e] | | 1.7 | | |
| $c_2$ | $\omega_1$ | 2.0 | | 2.0 | 2.0 |
| $c_2$ | $2^{1/4}\omega_1$ | 2.0 | | 2.0 | 2.0 |
| $c_2$ | $2^{1/2}\omega_1$ | 1.7 | | 2.7 | 3.0 |
| $c_2$ | $\{\omega\}$ [e] | | 2.3 | | |
| $c_3$ | $\omega_1$ | 2.3 | | 2.3 | 2.3 |
| $c_3$ | $2^{1/4}\omega_1$ | 2.3 | | 2.7 | 2.7 |
| $c_3$ | $2^{1/2}\omega_1$ | 2.0 | | 3.0 | 5.3 |
| $c_3$ | $\{\omega\}$ [e] | | 2.7 | | |

[a] Simulated model of table 1 with $\sigma$'s = 2, 3 and 5 $cm^{-2}$ at $\omega_1$.
[b] $\sigma_{A'} = 2.5\ cm^{-2}$ at $\omega_1$.
[c] Initial concentration ratios are 1:2:4.
[d] Normalized standard deviations for (1) unconstrained, (2) component-constrained, (3) $\omega$-constrained, and (4) $\omega, c$-constrained fits. Adequate discrimination occurs with $\omega, c$-constrained fits at highest speed.
[e] Combined speeds.

fits yielded n.S.D.'s of 1.7 or less, thus correctly indicating the consistency of the assumed model. Table 2 also indicates the advantage of column lengths longer than 0.36 cm. The 0.72 cm length has an extensive depleted region at all speeds that is, in a sense, unused. Reducing the speed to generate a minimum sigma of 1 $cm^{-2}$, however, offers no advantage, probably due to the lessened fractionation at these low speeds.

If separate estimations of the n.S.D. on each of the nine concentration distributions are made for the $\omega, c$-constrained fits, the concentration distributions at the highest speed usually have the largest n.S.D., probably because the highest speed affords the greatest fractionation. Although the n.S.D.'s for the lower speeds may be insufficient to discriminate association modes, it is the constraints imposed by the lower speed data that makes possible the discrimination at the higher speed. Which speed offers maximum discrimination depends upon the precise experimental parameters. If the higher speed causes most of the cell contents to be in the aggregated form, the intermediate speed, even though it results in less fractionation, may offer greater discrimination. Another factor determining discrimination of each channel is the maximum observable concentration, which is often greater at the lower speeds because of their smaller concentration gradients. Table 3 presents a more complete analysis of one simulated mixed association model from table 2. Single concentration distribution n.S.D.'s are presented for (1) unconstrained, (2) component constrained, (3) $\omega$-constrained, and (4) $\omega, c$-constrained fits. In this case, adequate discrimination does not occur unless the simulated experiment is performed at both a series of speeds and loading concentrations.

Table 4
Multi-speed analysis of histone f2a1 and f3 interaction [a]

| Speed | n.S.D. | | | |
|---|---|---|---|---|
| | $A + B \rightleftharpoons C$ [b] | | $2A' \rightleftharpoons C$ [c] | |
| | unconst. | $\omega$-const. | unconst. | $\omega$-const. |
| 28 000 rpm | 1.0 | 1.3 | 1.0 | 1.7 |
| 34 000 | 1.0 | 11.0 | 1.0 | 1.7 |
| 40 000 | 1.3 | 1.7 | 2.0 | 2.0 |
| Combined | | 6.3 | | 1.7 |

[a] Conditions are: loading concentrations of 0.25, 0.5 and 1 mg/ml; 0.1 M NaCl, 0.05 M NaOAc buffer, pH 5; 20°C.
[b] Model assumed is: $(f2a1)_2 + (f3)_2 \rightleftharpoons (f2a1)_2\ (f3)_2$.
[c] Model assumed is: $2\,(f2a1)\,(f3) \rightleftharpoons (f2a1)_2\,(f3)_2$.

The multi-speed fits were used to analyze the association of histone fractions f2a1 and f3 in order to distinguish the mixed and self-association modes of eqs. (3) and (4), respectively. A 12 mm external loading cell contained 0.34 cm columns of histone at 0.25, 0.5 and 1 mg/ml in 0.1 M NaCl, 0.05 M NaOAc buffer, pH 5. Rotor speeds of 28 000, 34 000 and 40 000 rpm, at 20°C, were used for the multi-speed analysis. Table 4 presents the n.S.D.'s for unconstrained and speed constrained fits assuming the mixed-association or self-association models. The unconstrained fits are incapable of discrimination. The multi-speed fit, however, eliminates the mixed-association and indicates that the self-association of two (f2a1) (f3) dimers to form the tetramer is the best model.

Another example of a sometimes ambiguous model is a monomer–dimer–tetramer self-association. If data are not available at sufficiently high concentrations for the tetramer to be the major species, this system may often closely resemble a monomer–trimer

Table 5
Multi-speed fit of monomer–dimer–tetramer system assuming monomer–trimer model [a]

| Initial conc. [b] | Speed | n.S.D. [c] | | | |
|---|---|---|---|---|---|
| | | 1 | 2 | 3 | 4 |
| $c_1$ | $\omega_1$ | 2.3 | | 4.3 | 4.3 |
| $c_1$ | $2^{1/4}\omega_1$ | 2.0 | | 3.7 | 3.7 |
| $c_1$ | $2^{1/2}\omega_1$ | 2.0 | | 5.7 | 4.7 |
| $c_1$ | $\{\omega_1\}$ [d] | | 4.3 | | |
| $c_2$ | $\omega_1$ | 2.3 | | 4.0 | 4.0 |
| $c_2$ | $2^{1/4}\omega_1$ | 1.7 | | 6.7 | 6.7 |
| $c_2$ | $2^{1/2}\omega_1$ | 2.0 | | 10.7 | 12.0 |
| $c_2$ | $\{\omega_1\}$ [d] | | 5.7 | | |
| $c_3$ | $\omega_1$ | 2.3 | | 5.0 | 5.0 |
| $c_3$ | $2^{1/4}\omega_1$ | 2.0 | | 6.0 | 6.0 |
| $c_3$ | $2^{1/2}\omega_1$ | 2.0 | | 14.3 | 15.0 |
| $c_3$ | $\{\omega\}$ [d] | | 6.0 | | |

[a] $\sigma_1 = 2.0$ at $\omega_1$; association constants are $K_2 = 1.0\ \text{mm}^{-1}$ and $K_4 = 1.5\ \text{mm}^{-3}$.
[b] Initial concentrations are 0.75, 1.5 and 3.0 mm fringe displacement.
[c] Normalized standard deviations for (1) unconstrained, (2) component-constrained, (3) $\omega$-constrained, and (4) $\omega, c$-constrained fits.
[d] Combined speeds.

self-association, A "two-species plot" will be apparently linear, to within experimental error, and consistent with monomer–trimer. Standard deviations of fits of the concentration distributions of imperfect (experimental or noise-perturbed simulated) data will be consistent with both monomer–trimer and monomer–dimer–tetramer models. Table 5 presents the results of a multi-speed analysis of a simulated monomer–dimer–tetramer system. The monomer sigma at the lowest speed is 2 $\text{cm}^{-2}$; the association constants on a weight concentration basis are $K_2 = 1.0\ \text{mm}^{-1}$ and $K_4 = 1.5\ \text{mm}^{-3}$; the total initial concentration is 1 mm fringe displacement; column length is 0.36 cm; and speed ratios are $1{:}2^{1/4}{:}2^{1/2}$. The single channel fits for the three speeds indicate the apparent consistency of the incorrect monomer–trimer model. The component constrained and $\omega$-constrained fits are powerful in eliminating this incorrect model. The discrimination is sufficient by means of the $\omega$-constrained fit (n.S.D. typically more than 10 for the highest speed) that it is probable that the multi-speed technique could often discriminate between the difficult alternatives: monomer–dimer–tetramer; monomer–trimer–tetramer; and monomer–dimer–trimer–tetramer. However, these cases have not yet been investigated.

In situations where the greater discrimination of the multi-speed technique is unnecessary to remove ambiguities in the association mode, the technique may nevertheless be of value in yielding more accurate association constants than are available from a single speed. Non-ideality has not been included in this discussion. The extension to non-ideal systems can be made by introducing non-linear fits with the second virial coefficient a parameter of the fit. Non-linear fits of equations of the form eq. (13) may be useful in cases where one or more of the sigmas are not previously assumed. The additional constraint on the problem would still be afforded from the simultaneous multi-speed fit, but the convenience of a linear fit would be lost. In any case, the work presented here for analyzing interacting systems of discrete species, and the work of Scholte (3) for obtaining a distribution function for non-interacting, broadly heterogeneous systems, both demonstrate the advantage of combining in a single fitting procedure the data from experiments at a series of rotor speeds (and initial concentrations). It is probably only in this manner that the ambiguities inherrent in analyzing a sum of several exponentials can be resolved.

## 5. Overspeeding

The time required to essentially obtain sedimentation equilibrium at some angular velocity $\omega_{eq}$ can be substantially reduced by temporarily overspeeding at velocity $\omega_{os}$ [12–14]. The optimal overspeed time depends upon all parameters determining the equilibrium distribution at $\omega_{eq}$ and upon the overspeed $\omega_{os}$. Indeed, Teller [14] demonstrated the necessity of a careful choice of overspeed time, which if excessive could increase the total time required to reach equilibrium. The overspeed calculations involve lengthy series approximations of the Lamm equation for the rectangular case. The most thorough study is that of Teller [14] who used sufficient terms in the approximation to justify application to high-speed equilibrium experiments. An overspeeding procedure based

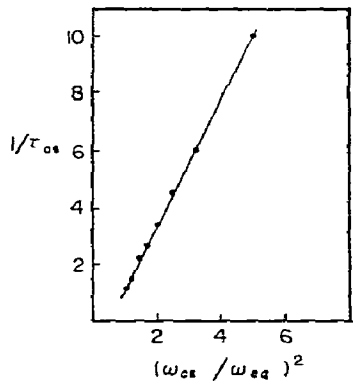


Fig. 5. Optimal reduced overspeed time. Reciprocal overspeed times are presented as a function of the overspeed ratio $(\omega_{os}/\omega_{eq})$.

upon the calculations of Teller has proven useful in our laboratory. The procedure is to some extent empirical. It is presented here with no further justification than its apparent usefulness, and to encourage more complete mathematical analyses of overspeeding. Along with Teller, we define the reduced overspeed time $\tau_{os}$ as

$$\tau_{os} \equiv t_{os}\, s\, \omega_{eq}^2\, \bar{r}/(r_b - r_m), \tag{27}$$

where $t_{os}$ is the overspeed time in seconds; $r_m$ and $r_b$ are the meniscus and base radial positions; and $\bar{r}$ is the midpoint. Teller presented values of the optimal $\tau_{os}$ required to minimize the total time required to essentially attain equilibrium. He used an alternative reduced molecular weight $H$:

$$H = \sigma(r_b^2 - r_m^2)/4. \tag{28}$$

$H$ and $\sigma$ correspond to speed $\omega_{eq}$. The extension made here is to note that the simulated data for the optimal $\tau_{os}$ presented by Teller can be approximated by

$$\tau_{os} = \frac{0.267\, H^{0.58}}{(\omega_{os}/\omega_{eq})^2 - 1/2}. \tag{29}$$

The dependence on the overspeed ratio $(\omega_{os}/\omega_{eq})$ is particularly simple, and implies that a presentation of $1/\tau_{os}$ as a function of the square overspeed ratio should be linear. Fig. 5 presents values of $\tau_{os}$ obtained as the minima of the family of curves in Teller's fig. 4. The linearity is essentially perfect. The dependence of $\tau_{os}$ upon $H$ corresponds to that of eq. (29) at least near the conditions of a typical high-speed sedimentation equilibrium experiment.

Eqs. (27) and (29) may be combined to yield the optimal overspeed time in seconds:

$$t_{os} = \frac{0.0814\,(\Delta r)^{1.58}}{[(\omega_{os}/\omega_{eq})^2 - 1/2]}\,\frac{\sigma^{0.58}}{s\,\omega_{eq}^2}, \tag{30}$$

where $\Delta r$ is $(r_b - r_m)$ and $\bar{r} = 6.5$ cm. The overspeed time $t_{os}$ depends upon both $\sigma$ and $s$, which in turn depend upon the molecular weight and frictional coefficient $f$,

$$s = M(1 - \bar{v}\rho)/Nf. \tag{31}$$

Thus, $t_{os}$ is linearly proportional to the frictional coefficient, which is generally unknown in a sedimentation equilibrium experiment. However, a minimum frictional coefficient, $f_0$, may be calculated from Stoke's formula assuming an unhydrated compact sphere of molecular weight $M$ and partial specific volume $\bar{v}$:

$$f_0 = 6\pi\eta(3\bar{v}M/4\pi N)^{1/3}. \tag{32}$$

$\eta$ is the solvent viscosity and $N$ Avogadro's number. Since $f > f_0$, use of eq. (32) yields a conservative estimate of the overspeed time. A less than optimal overspeed time results in some savings of total time required for equilibrium; while an excessive overspeed time risks an actual increased equilibrium time compared to no overspeeding. A better estimate of $f$ is made by multiplying eq. (32) by a reasonable estimate of the frictional ratio $(f/f_0)$.

Combination of eqs. (27), (30)–(32) yields

$$t_{os} = \frac{1.73 \times 10^{11}}{M^{0.09}\omega_{eq}^{0.84}\,[(\omega_{os}/\omega_{eq})^2 - 1/2]} \times \left[\left(\frac{f}{f_0}\right)\frac{\eta\bar{v}^{1/3}\,(\Delta r)^{1.58}}{(1-\bar{v}\rho)^{0.42}\,T^{0.58}}\right]. \tag{33}$$

In practice, the smallest $(f/f_0)$ observed in protein experiments is 1.14. It is convenient to define a correction factor $\theta$, which for a "standard" aqueous high-speed experiment has a value of unity when,

$f/f_0 = 1.14$, $\quad \bar{v} = 0.73$ cc/g, $\quad \Delta r = 0.3$ cm,

$\rho = 1$ g/cc, $\quad T = 293$ K.

Table 6
Overspeed times for standard systems[a)]

| M.W. | $rpm_{eq}$ | $rpm_{os}$ | $t_{os}$ (minutes) |
|---|---|---|---|
| 15 000 | 52 000 | 56 000 | 101 |
| 40 000 | 30 000 | 44 000 | 66 |
| 40 000 | 30 000 | 36 000 | 115 |
| 80 000 | 20 000 | 28 000 | 98 |
| 80 000 | 20 000 | 24 000 | 152 |
| 200 000 | 14 000 | 20 000 | 115 |
| 200 000 | 14 000 | 16 000 | 220 |

[a)] With $\theta = 1$, for typical high-speed sedimentation equilibrium experiments.

$$\theta = \left(\frac{f/f_0}{1.14}\right)\left(\frac{\Delta r}{0.3}\right)^{1.58}\left(\frac{\eta}{\eta_{20,w}}\right)\left(\frac{0.27}{1-\bar{v}\rho}\right)^{0.42} \times \left(\frac{\bar{v}}{0.73}\right)^{1/3}\left(\frac{293}{T}\right)^{0.58}. \quad (34)$$

With this definition, and with $t_{os}$ in minutes and rotor speeds in rpm, the optimal overspeed time (in minutes) is

$$t_{os} = \frac{1.62 \times 10^6\,\theta}{M^{0.09}(rpm_{eq})^{0.84}[(rpm_{os}/rpm_{eq})^2 - 1/2]}. \quad (35)$$

The feature of eq. (35) which makes it potentially useful is the only slight dependence upon the molecular weight. If precise a priori knowledge of $M$ were required, accurate estimation of $t_{os}$ would usually be impossible. However, variation to the 0.09 power permits considerable uncertainty in $M$ and permits overspeeding of polydisperse systems. We may enquire intuitively for the reason of this slight dependence. For a given overspeed time, a high molecular weight species sediments more towards the cell base than does a low molecular weight species. But at sedimentation equilibrium, the larger species is distributed more towards the cell base. Thus, we would not expect a great variation of the optimal $t_{os}$ with molecular weight. The central difficulty in estimating $t_{os}$ is not prior knowledge of $M$, but estimation of the frictional ratio. If $(f/f_0)$ is unknown, it is assumed equal to 1.14, as in eq. (35), to estimate a less than optimal $t_{os}$.

The choice of the overspeed ratio $(\omega_{os}/\omega_{eq})$ determines the extent of time reduction possible by overspeeding. For a typical high-speed experiment, the optimal overspeed ratio is near $\sqrt{5}$ and results in approximately a sevenfold reduction of total time. An overspeed ratio of $\sqrt{2}$ should yield a threefold reduction in time. High overspeed ratios, particularly in high-speed sedimentation equilibrium experiments, may result in gel formation at the cell base with a consequent slow approach to equilibrium. An overspeed ratio of $\sqrt{2}$ is preferable to higher ratios; and in the case of anticipated equilibrium $\sigma$'s in excess of 8 $cm^{-2}$, even more moderate overspeeding should be employed. Table 6 presents overspeed times for typical systems with $\theta = 1$.

If equilibrium at speed $\omega_2$ is approached from a previously attained equilibrium at a lower speed $\omega_1$, eq. (35) overestimates the overspeed time at some third speed $\omega_3$. Charlwood [15] and Wilcox and Spragg [16] have examined the approach to equilibrium from a lower speed. However, their treatments are not directly applicable to the overspeed problem. On an empirical basis, our lab modifies eq. (35) by multiplying the expression by $\theta'$:

$$\theta' = 1 - (rpm_1/rpm_2)^2. \quad (36)$$

Eq. (36) has the correct limiting behavior as $rpm_1$ approaches either zero or $rpm_2$.

The overspeed considerations given here are at present intended to be of modest utility in reducing times required for sedimentation equilibrium experiments. The reductions are particularly appreciated in the multi-speed experiments, discussed earlier, where equilibrium is attained at three speeds. Inadvertantly exceeding the optimal overspeed time is not likely to result in an actual increased time to reach equilibrium, compared with no overspeeding, if eq. (35) is used. For the cases presented by Teller [14], with an overspeed ratio of $\sqrt{2}$, time reduction is afforded by all overspeed times less than 1.7 times the optimal $t_{os}$. Future work, particularly additional computer simulations of the series solutions to the Lamm equation, will be needed to explore the validity of the approximate eqs. (35) and (36).

**Acknowledgement**

This work is supported in part by USPHS, NIH grant GM 18456.

## References

[1] D.A. Yphantis, Biochemistry 3 (1964) 297.
[2] R.H. Haschemeyer and W.F. Bowers, Biochemistry 9 (1970) 435.
[3] Th.G. Scholte, Ann. N.Y. Acad. Sci. 164, Art. 1 (1969) 156.
[4] D.E. Roark, T.E. Geoghegan and G.H. Keller, Biochem. Biophys. Res. Comm. 59 (1974) 542.
[5] R.D. Kornberg and J.O. Thomas, Science 184 (1974) 865.
[6] D.E. Roark and D.A. Yphantis, Ann. N.Y. Acad. Sci. 164, Art. 1 (1969) 245.
[7] R.J. Delange, D.M. Fambrough, E.L. Smith and J. Bonner, J. Biol. Chem. 244 (1969) 319 and 5669.
[8] R.J. Delange, J.A. Hooper and E.L. Smith, Proc. Nat. Acad. Sci. USA 69 (1972) 882.
[9] R.M. Carlisle, J.I.H. Patterson and D.E. Roark, Analyt. Biochem. 61 (1974) 248.
[10] A.T. Ansevin, D.E. Roark and D.A. Yphantis, Analyt. Biochem. 34 (1970) 237.
[11] F.B. Hildebrand, Introduction to Numerical Analysis (McGraw–Hill, New York, 1956).
[12] P.E. Hexner, L.E. Radford and J.W. Beams, Proc. Nat. Acad. Sci. USA 47 (1961) 1848.
[13] E.G. Richards, D.C. Teller and H.K. Schachman, Biochemistry 7 (1968) 1054.
[14] D.C. Teller, T.A. Horbett, E.G. Richards and H.K. Schachman, Ann. N.Y. Acad. Sci. 164, Art. 1 (1969) 66.
[15] P.A. Charlwood, Can. J. of Biochem. 46 (1968) 845.
[16] J.K. Wilcox and S.P. Spragg, Re-attainment of Sedimentation Equilibrium, paper in preparation.